Table 1. Patient Characteristics

Characteristics	No of Patients	%
Sex		
Male	19	70.4
Female	8	29.6
Age, years		
Mean (SD)	52.6 (24.7)	
Range		27day-89y
Underlying disease		
Solid malignant neoplasia	7	25.9
Leukemia	5	18.5
Renal failure	4	14.8
Inflammatory liver disease	3	11.1
Cerebral hemorrhage	2	7.41
Gastric ulcer	1	3.7
Congenital duodenal atresia	1	3.7
Necrotising fascitis	1	3.7
Arrythmia	1	3.7
Multiple organ failure	1	3.7
Acute respiratory distress syndrome	1	3.7
Therapy		
Antibacterial drug	17	62.9
Steroid	8	29.6
central venous catheterization	13	48.1
Blood culture		
Positive	11	40.7
Negative	16	59.3

5.6 ± 2.9.

2-3. Distribution and morphometric analysis of the lesions

From the observation of computer-processed images of CNS schema in which all candidial lesions were plotted (Fig. 2), 23 cases had supratentorial lesions, 20 had brain stem lesions, and 7 cases had cerebellar lesions. Among these, 13 cases had lesions both in the supratentorial region and in brain stem, and 3 cases had lesions in the entire brain (supratentorial, cerebellar, and brain stem regions). In contrast, only one case and none had lesions limited to the brain stem and cerebellum, respectively (Fig. 3). In addition, 23 cases had lesions in the supratentorial region showed no predilection in distribution of their lesions (Fig. 4).

The density and mean area of the lesions in each region were, respectively: supratentorial gray matter, 2.70 ± 4.75 lesions/cm^2 and 0.0863 ± 0.0059 mm^2; supratentorial white matter, 0.91 ± 1.06 lesion/cm^2 and 0.3572 ± 0.0332 mm^2; basal ganglia, 0.49 ± 1.18 lesion/cm^2 and 0.1541 ± 0.0031 mm^2; brain stem, 0.54 ± 0.91 lesion/cm^2 and 0.129 ± 0.0021) mm^2; and cerebellum, 0.07 ± 0.16 lesion/cm^2 and 0.1252 ± 0.0019 mm^2 (Fig. 5 and 6).

The total number of supratentorial lesions was 688 lesions, the mean distance between the brain surface and the lesion was 4.026 ± 3.159 mm (Fig. 7). The mean distances between the brain surface and the lesion in cases with bacterial, aspergillus, and zygomycetes infection were 5.340 ± 5.076 mm (n=152), 0.460 ± 0.395 mm (n=14), and 3.130 ± 3.076 mm (n=18), respectively. Thus, candidial lesions tended to be more superficial than bacterial lesions and deeper than filamentous fungal lesions (bacteria: $P < 0.001$, asper-

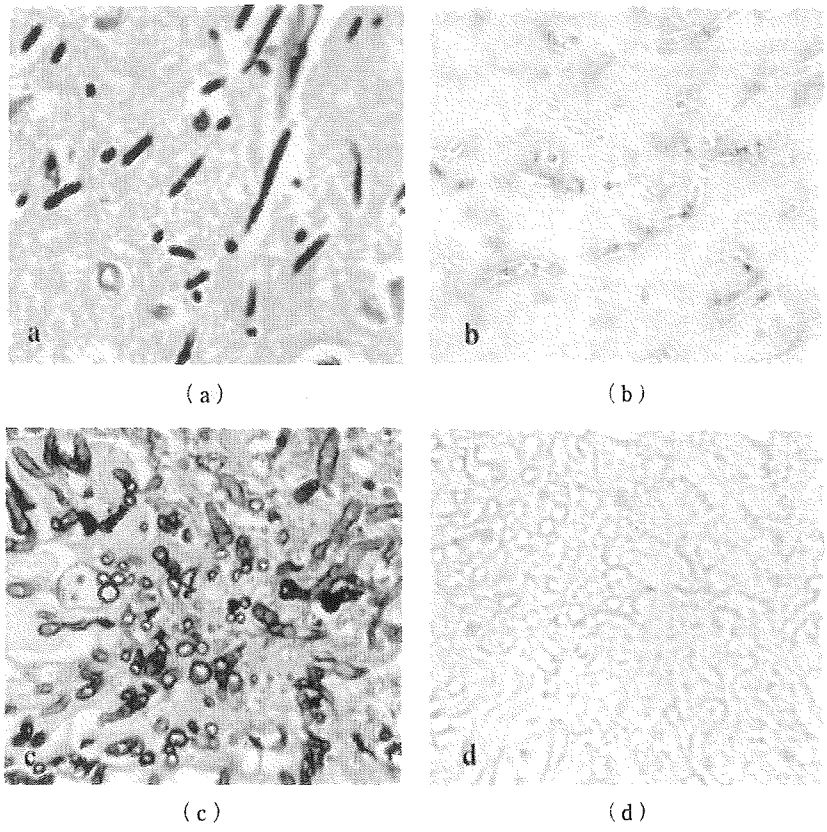

Fig. 1. Shape of *Candida* in CNS lesion with identification by ISH. a: Pseudohyphal growth of *Candida* in tissue section (PAS stain, x400), b: *Candida* shows distinct signal recognized as cluster of fine black dots by PNA-ISH (PNA-ISH with *Candida*-specific PNA probe, x400), c: Pseudohyphal growth of *Trichosporon* in tissue section (PAS reaction, x400), d: *Trichosporon* is negative for PNA-ISH (PNA-ISH with *Candida*-specific PNA probe, x400).

gillus: $P < 0.001$, zygomycete: $P < 0.05$) (Fig. 8).

2-4. Tissue responses

Three major histological findings were analyzed: yeast cell proliferation, infiltration of neutrophils, and response of macrophages. These were graded as absent, mild or negligible, and extensive or prominent (indicated as 0, 1, and 2). Their representative findings are shown in Figure 9. As a result, most tissue responses could be classified into four patterns: yeast cell predominant (excess candidial proliferation without inflammatory infiltrate), neutrophil predominant (dense neutrophil infiltration with negligible yeast cell proliferation), macrophage depletion (prominent candidial proliferation and neutrophil infiltration), and competitive type (competes with candidal proliferation, neutorophil infiltration, and macrophage infiltration) (Fig.10).

Discussion

The candidial blood stream infection is one of the most critical invasive fungal infections and has a particularly high mortality when the CNS is involved. It has been reported that a delay in the initiation of fluconazole therapy in hospitalized patients with candidemia significantly affects mortality. Therefore, new methods to avoid delays in appropriate antifungal therapy, such as rapid diagnostic tests or identification of unique risk factors, are needed[15,16]. Given these circumstances, the present study aims to elucidate specific pathophysiological characteristics of CNS candidiasis that may be instrumental in developing a procedure for early diagnosis.

We, first of all, extracted 27 autopsy cases of systemic candidiasis, 10 of bacterial infection, 5 of aspergillosis and zygomycosis. *Candida* spp. that had previously been identified by histological observation in all 27 cases were

Table 2. Summary of histological findings of Organs Involved in Cases of Candidiasis

Case ＼ Organ	Brain	Kidney	Lung	Heart	TG	Liver	Eso	Spleen	Sint	Dia	Sto
1	+	+	+	+	+	-	-	+	-	-	-
2	+	+	+	+	+	-	-	-	-	-	-
3	+	+	+	-	+	-	+	-	+	-	-
4	+	+	+	+	-	-	-	-	-	-	-
5	+	+	+	+	+	+	-	-	-	-	-
6	+	+	+	+	-	+	-	-	-	-	-
7	+	+	+	+	+	-	-	-	-	-	-
8	+	+	+	+	+	-	-	-	-	-	-
9 *	+	N	N	N	N	N	N	N	N	N	N
10	+	+	+	+	-	-	-	-	-	-	-
11	+	+	+	+	-	-	+	-	-	-	-
12	+	+	+	+	-	-	-	-	-	-	-
13	+	+	+	+	-	+	+	-	+	-	-
14	+	+	+	+	+	+	-	-	-	-	-
15	+	-	+	+	+	-	-	-	-	+	-
16	+	+	+	+	+	+	-	+	-	+	+
17	+	+	+	+	-	-	-	-	-	-	-
18	+	+	+	-	-	-	-	-	-	-	-
19	+	+	+	-	-	-	-	-	-	+	+
20	+	+	-	-	-	-	-	-	-	-	-
21	+	+	+	+	-	-	-	-	-	-	-
22	+	+	+	+	+	-	-	-	-	-	-
23	+	-	+	+	+	-	-	-	-	-	-
24	+	+	-	+	-	-	-	-	-	-	-
25	+	+	+	+	+	+	-	+	+	-	+
26	+	+	+	+	-	+	+	-	-	-	-
27	+	+	-	-	-	-	-	-	-	-	-
Number of case	26/26	24/26	23/26	21/26	12/26	7/26	4/26	3/26	3/26	3/26	3/26
n = 26 (%)	100%	92.3%	88.5%	80.8%	46.2%	26.9%	15.4%	11.5%	11.5%	11.5%	11.5%

Abbreviations

- = not demonstraited; + = demonstrated; N = Not examined.

TG = Thyroid gland; Eso = Esophagus; Sint = Small intestine; Dia = Diaphragm; Sto = Stomach; Musc :

* = The autopsy had been limited in the brain.

identified as *C. albicans* by the PNA-ISH. Sensitive and rapid molecular detection assays have been introduced using the polymerase chain reaction (PCR), but most of these lack satisfactory specificity (i.e., have a high rate of false positive results)[17]. To address these problems, we attempted to detect *C. albicans*-specific nucleic acids in formalin-fixed and paraffin-embedded tissue sections of the CNS using ISH with a PNA probe targeting the rRNA of *C. albicans*. Other reported studies have used ISH with DNA probes to identify fungi in formalin-fixed and paraffin-embedded sections: however few have used PNA probes. This mimics with uncharged, neutral backbones that provide improved hybridization characteristics, such as high specificity, strong affinity, rapid kinetics, and an ability to hybridize to highly structured targets such as rRNA[18,19]. In addition, the relative hydrophobicity of PNA probes compared to DNA probes enables the former to penetrate the hydrophobic cell wall following preparation of a standard tissue section[20]. ISH with PNA probes that target rRNA is a novel techniqueitem that combines the unique performance characteristics of PNA probes with the advantages of using rRNA as a target. It has been used to identify cultures of both yeasts and bacteria[21,22], including identifying *Staphylococcus aureus* directly from blood culture bottles[23]. In the study described here, we

Musc	AG	GB	Pleura	BM	PG	GG	Blad	Mes	LN	Total
-	-	-	-	-	-	-	-	-	-	6
+	-	-	-	-	-	-	-	-	-	6
-	-	-	-	-	-	-	-	-	-	6
-	-	-	-	-	-	-	-	-	-	4
-	-	-	-	-	-	-	-	-	-	6
-	-	-	-	-	-	-	-	-	-	5
-	-	-	-	-	-	-	-	-	-	5
-	-	-	-	-	-	-	-	-	-	5
N	N	N	N	N	N	N	N	N	N	N
-	-	-	+	-	-	N	-	-	-	5
-	-	-	-	-	-	-	-	-	-	5
-	-	-	-	-	-	-	-	-	-	4
-	-	-	-	-	-	-	-	-	-	7
-	-	+	-	-	-	+	-	-	-	8
-	-	-	-	-	-	-	-	-	-	5
+	+	+	-	+	+	-	+	+	+	17
-	-	-	-	-	-	-	-	-	-	4
-	+	-	-	-	-	-	-	-	-	4
-	-	-	+	-	-	-	-	-	-	6
-	-	-	-	-	-	-	-	-	-	2
-	-	-	-	-	-	-	-	-	-	4
-	-	-	-	-	-	-	-	-	-	5
-	-	-	-	-	-	-	-	-	-	4
-	-	-	-	-	-	-	-	-	-	3
-	-	-	-	+	-	-	-	-	-	10
-	-	-	-	-	+	-	-	-	-	7
-	-	-	-	-	-	-	-	-	-	2
2/26	2/26	2/26	2/26	2/26	2/26	1/26	1/26	1/26	1/26	
0.08%	0.08%	0.08%	0.08%	0.08%	0.08%	0.04%	0.04%	0.04%	0.04%	

=Muscle; AG = Adrenal gland; GB = Gallbladder; BM = Bbone marrow; PG = Prostate gland; GG = Gonadal gland (testis/ovary); Blad = Bladder; Mes = Mesenterium; LN = Lymph node.

employed the PNA probe that targets *C. albicans* 26S rRNA and thus specifically identified *C. albicans* in paraffin-embedded and formalin-fixed tissue sections. In addition, PNA-ISH successfully shortened the hybridization time to detect the targeting nucleic acid from overnight to 90 minutes. This result suggests that PNA-ISH is a valuable supportive tool for rapid and accurate histopathological diagnosis of invasive candidiasis.

Except for one case, wherein only the brain was examined, we found *Candida* invasion in 5.6 organs on average (SD: 2.9) in each of the other 26 cases. This suggests that lesions of candidiasis form in the CNS when *Candida* infection has already spread in the body.

A previous study revealed that the blood flow rates in the cerebral cortex and white matter regions, as determined by a static xenon-enhanced CT approach, were 44.0 ± 7.1 m*l*/100 g/min and 24.3 ± 4.3 m*l*/100 g/min, respectively[24]. It was predicted that development of lesion in CNS candidiasis occurs more frequently in the cerebral cortex, this area having a higher blood flow than the medulla. We then examined the distribution of brain lesions in each case. The lesions were found most frequently in the supratentorial region (23 cases out of 27), predominantly in the cerebral grey matter and cerebral white matter. We next investigated susceptible sub-regions in the supratentorial region. To

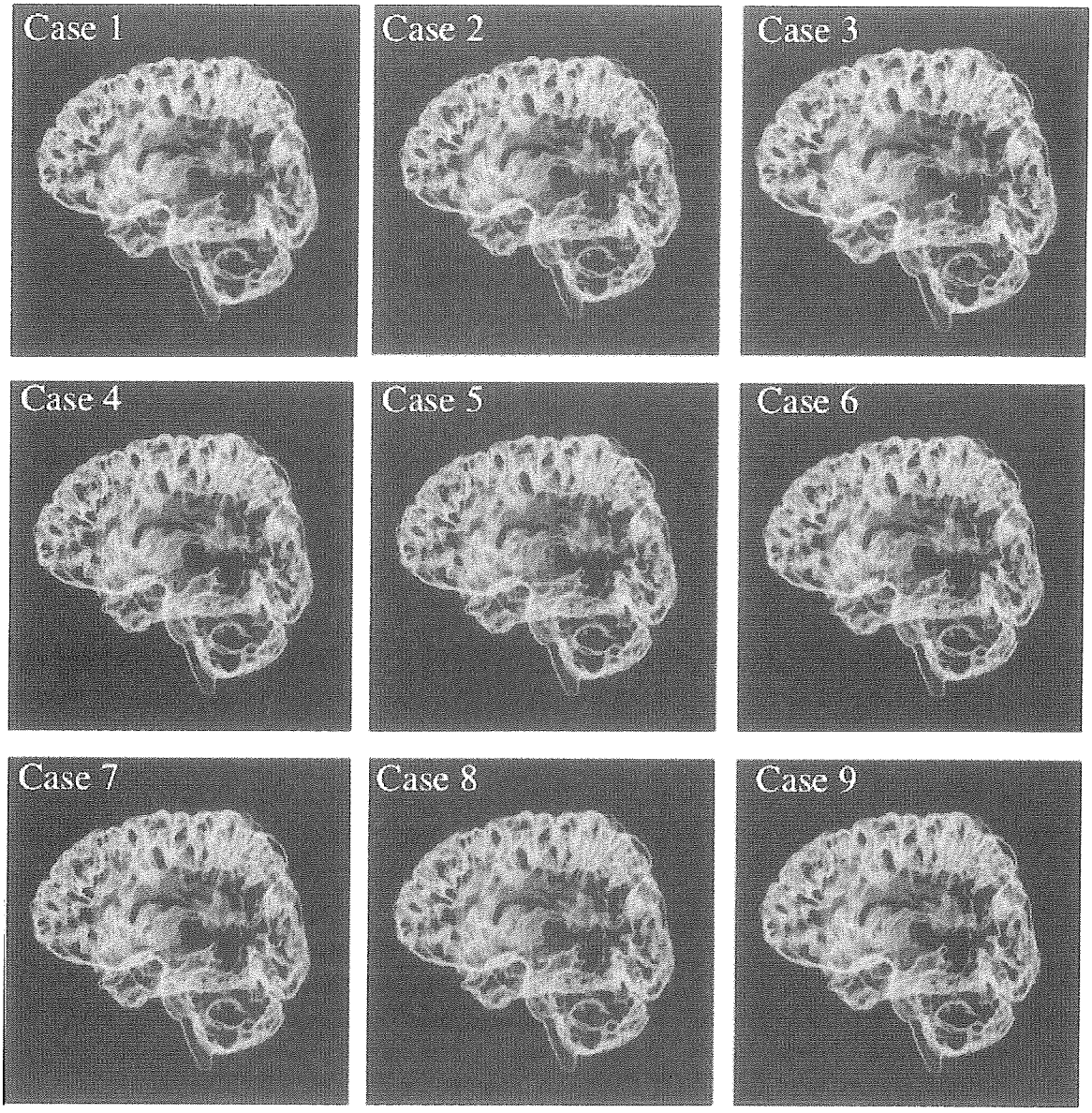

Fig. 2. Reconstruction of the Three-dimensional Structure of central nervous system candidiasis. (Case 1～Case 9)

adjust limitation in the size of the field used for observation, we evaluated the density of lesions formed in each sub-region. The average area ratio of a sub-region to the lesions in the corresponding sub-region observed in specimens was highest in the cortex, followed by the medulla, basal ganglia, brain stem, and cerebellum. These data clearly indicate that lesions of candidiasis are mainly formed in the cerebral cortex in the supratentorial region.

The further examination revealed that the distance between the centre of a lesion and the surface of the brain was 4.026 mm on average (SD: 3.159 mm), indicating that *Candida* lesions are mainly formed in the deep layer of the cerebral cortex in the supratentorial region. It was previously reported that lesions in CNS candidiasis frequently occurs in the corticomedullary junction[25]; but, no study has discussed relationship between normal structure of vessels and establishment of lesions. A time-course study of candidial endophthalmitis using experimental animals, performed by Omuta *et al.*, demonstrated that the sites of the primary lesions were concentrated in the near-equator area where tortuous small blood vessels are present, and suggested that such anatomical characteristics and consequent changes in blood flow may contribute to *Candida* colonization[26]. Tissue-specific vascular architecture and changes in blood flow were therefore suggested to be essential factors involved in *Candida* colonization, as

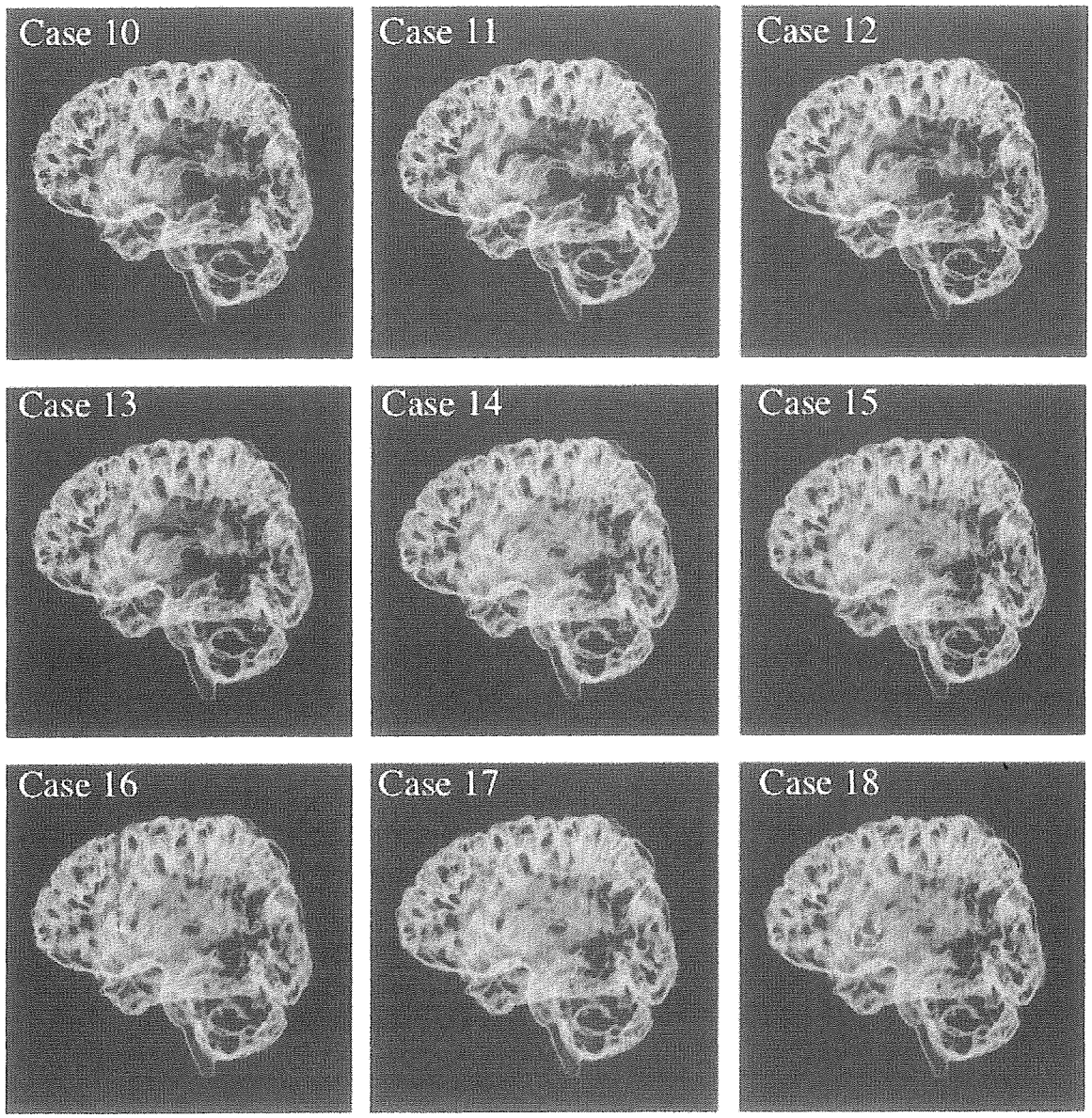

Fig. 2. Reconstruction of the Three-dimensional Structure of central nervous system candidiasis. (Case 10~Case 18)

well as in the formation and distribution of lesions. With respect to vascular architecture in the cerebrum, Akima *et al.* pointed out that the density of arteries gradually increases from the most upper to the deepest layer of the cerebral cortex[24,25]. In these studies, "fountain-like vascular branching" architecture was highlighted as deep-layer specific vascular architecture that represents the laminar structure of neurons in the cerebral cortex. In this unique architecture, many fine streams branch off a single artery mimicking sprays of water coming out from a fountain, that is, the artery branches out in anterograde or orthogonal directions at the primary branch point, while in retrograde directions towards the upper layer in the secondary and tertiary branch points. Interestingly, in the present study, it was found close to the lesions of candidiasis in the deep cortical layer, the area situated approximately 4 mm below the surface of the brain, suggesting some involvement of the "fountain-like vascular branching" architecture in colonization, lesion formation and lesion distribution of *C. albicans* in the cerebrum. Also, *Candida* adhesion onto the vascular endothelium, a step prior to tissue colonization, always occurs in the presence of blood flow[26], and *Candida* may adhere onto the vascular endothelium upon receiving distorting force generated by shear stress attributed to blood flow. Therefore, it was considered that changes in blood flow, increasing in shear stress on the vascular endothelium

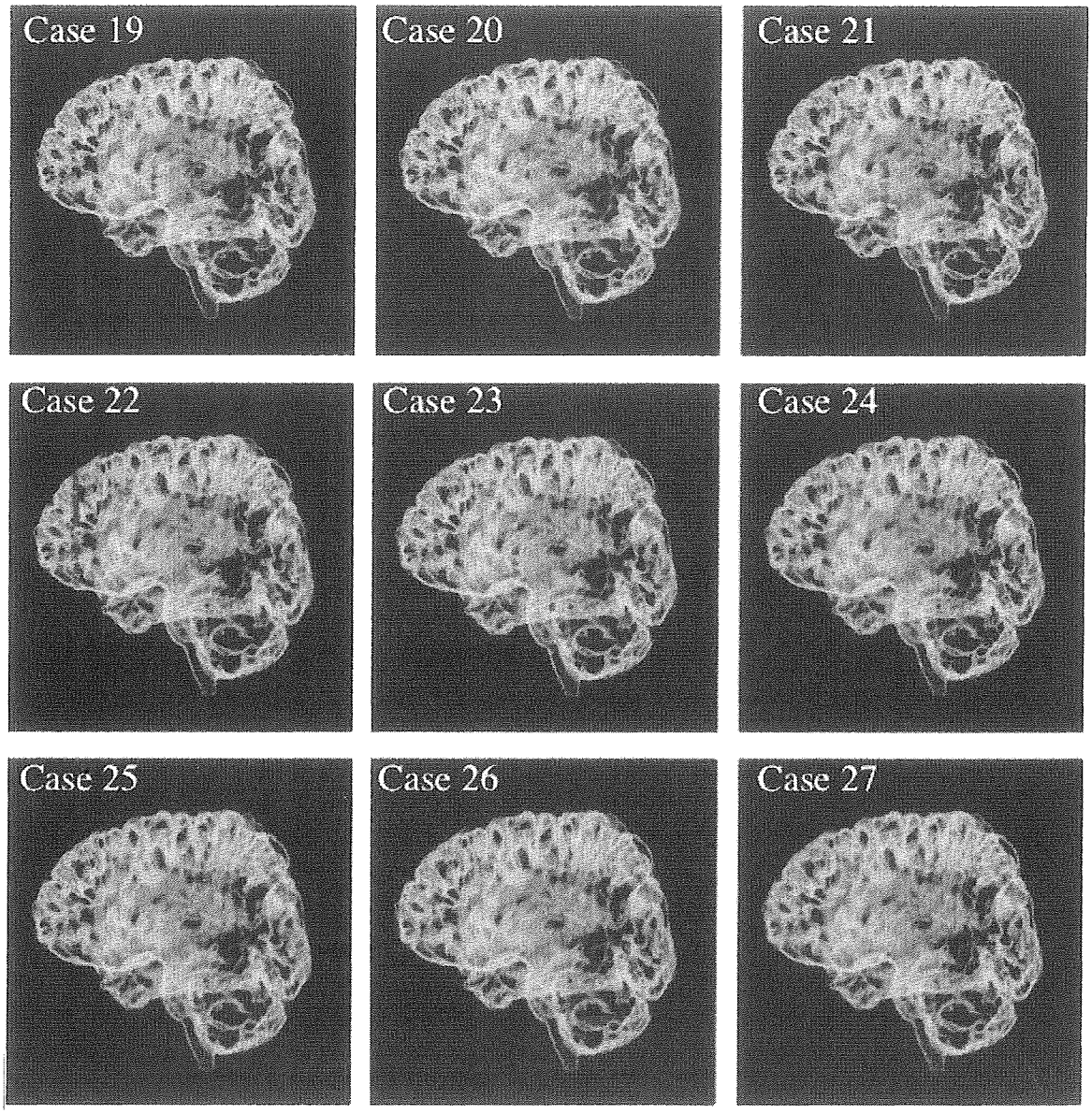

Fig. 2. Reconstruction of the Three-dimensional Structure of central nervous system candidiasis. (Case 19~Case 27)

and generating distortional flow play important roles in colonization as an initial event for development of candidial lesion in the cerebrum. Furthermore, when the distribution of candidial lesions in the CNS was statistically compared with those of other deep mycoses (e. g., aspergillosis and zygomycosis) and bacterial infections, as determined by a similar approach, the sites of candidial lesions in the CNS were significantly deeper from the surface of the brain than those of other fungal lesions, but were significantly closer to the surface than those of bacterial lesions. Therefore, the site of the lesions determined in this study appeared specific for *Candida*. Moreover, when the average sizes of all lesions observed in the sub-regions (e.g., grey matter, white matter and basal ganglia) of the supratentorial region on the specimens were compared, the lesions formed in white matter tended to be larger than those formed in the cortex and basal ganglia. A mechanism underlying this tendency is possibly similar to that underlying the spread and extension of bleeding and tumors in the cerebrum towards the relatively susceptible white matter, but not towards the grey matter which is resistant to invasion[31].

Clinically, since the indication of open brain biopsy is limited, multislice CT with excellent spatial resolution (in the range from 0.23 mm to 0.50 mm) and low contrast resolution MRI are believed to be effective approaches for demonstrating microlesions formed in

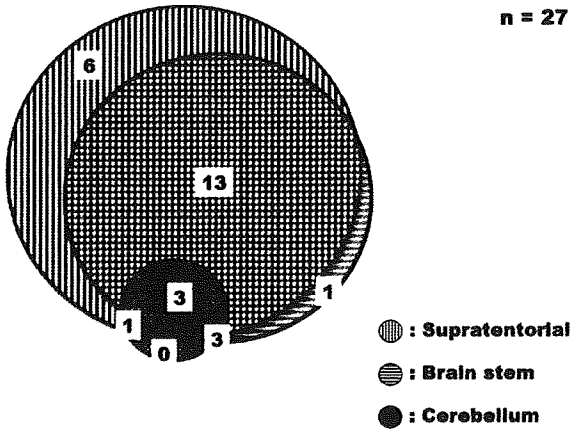

Fig. 3. The distribution of foci of *Candida* infection in CNS with Venn diagram.

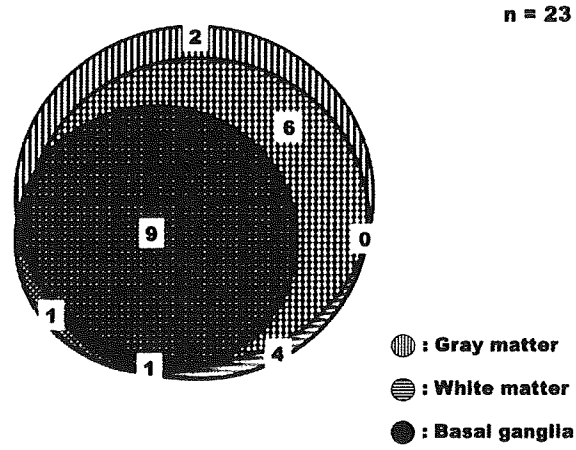

Fig. 4. The distribution of supratentorial lesion with Venn diagram.

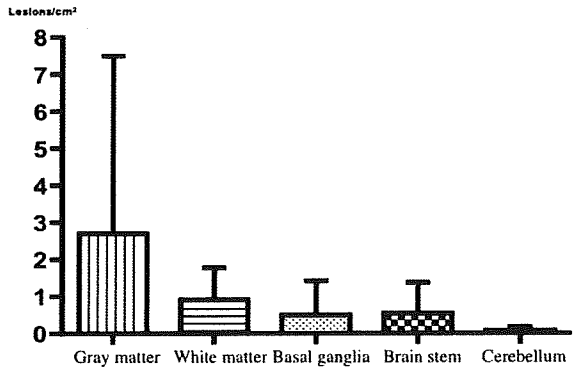

Fig. 5. Comparison of the density of lesions in different areas.

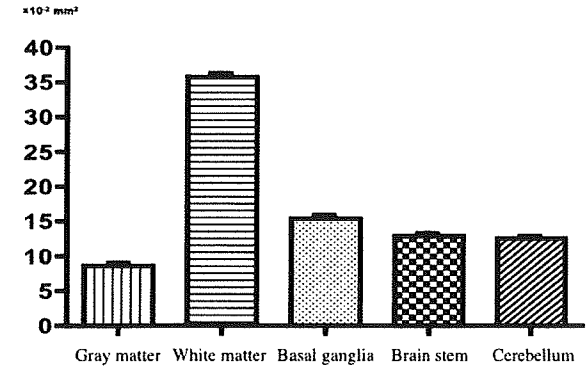

Fig. 6. Comparison of the mean area in different areas.

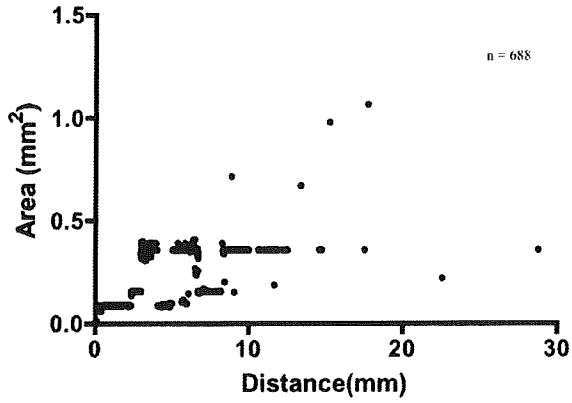

Fig. 7. Scatter plot of Area and Distance about *Candida* infectious lesions in CNS.

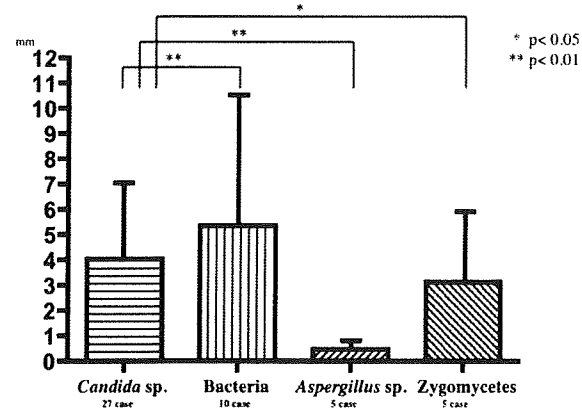

Fig. 8. Comparison of mean distance between the lesion and the brain surface in cases with *Candida* spp, bacteria, *Aspergillus* spp, and Zygomycetes.

the CNS inside the skull[31]. We found that lesions in CNS candidiasis, of which the average size was 0.0863 mm^2, frequently formed in the cortical white matter situated approximately 4 mm below the surface of the brain. Taken together. we would like to highlight a possible diagnosis of CNS candidiasis based on a radiological approach that examines lesions shown in thin-slice images of the relevant area (approximately 4 mm below the surface of the brain) created by high-resolution imaging techniques.

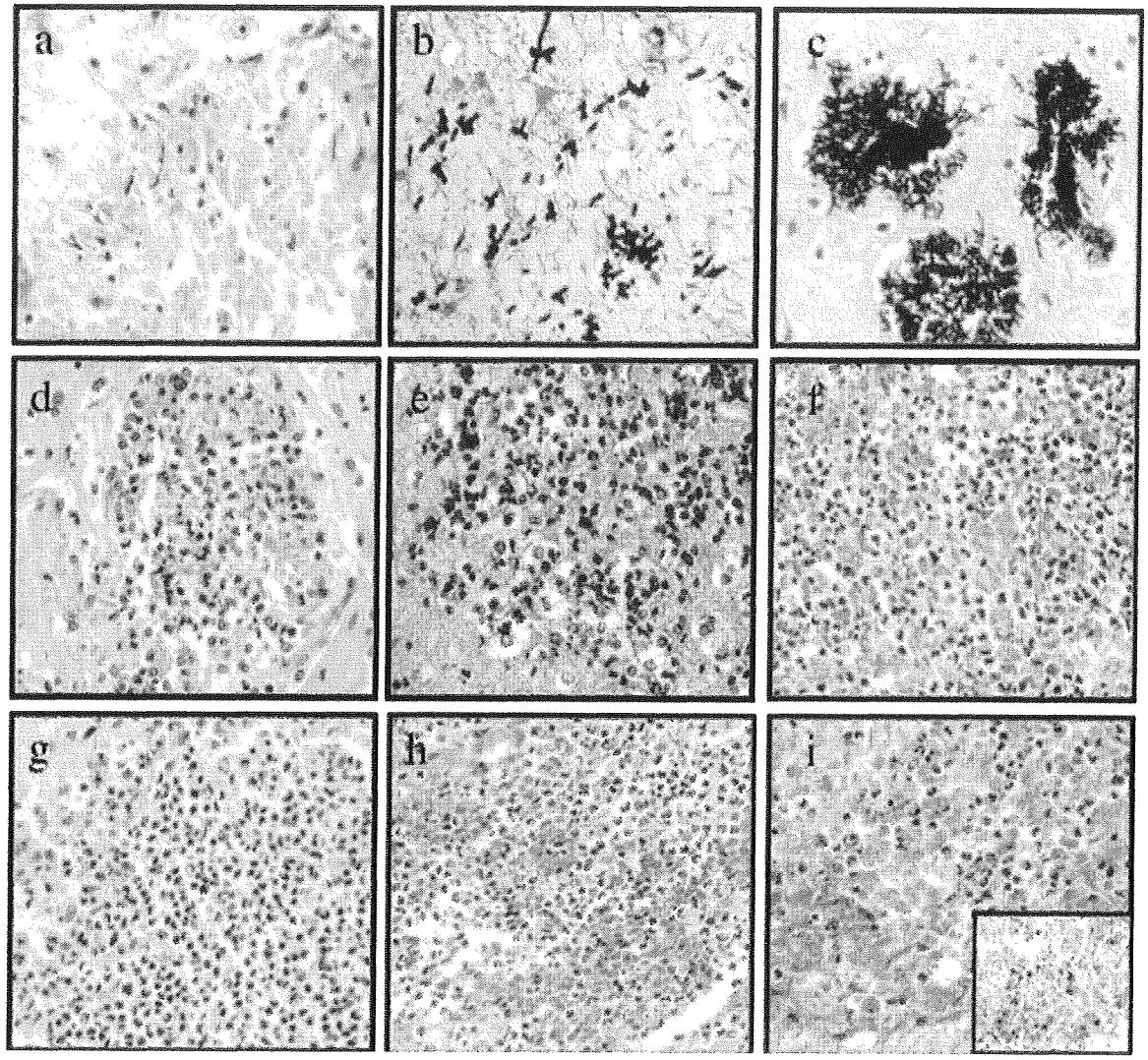

Fig. 9. Representative histological findings.
(a) The degree of the yeast cell proliferation 1
(b) The degree of the yeast cell proliferation 2
(c) The degree of the yeast cell proliferation 3
(d) The degree of the neutrophil infiltration1
(e) The degree of the neutrophil infiltration 2
(f) The degree of the neutrophil infiltration 3
(g) The degree of the macrophage response 1
(h) The degree of the macrophage response 2
(i) The degree of the macrophage response 3
(a, b, and c: PAS stain, d, e, f, g, h, and i: Hematoxylin & Eosin stain, Inset of i: Immunostain with CD68, x400).

Histological findings of the foci of pathogenic microorganisms represent the response of host defence mechanism. In particular, shape of *Candida* in the tissue of patients with invasive fungal infections can be examined in detail, as well as expansion of necrosis and infiltration of inflammatory cells. These findings are believed to be common to typical invasive fungal infections, such as candidiasis and aspergillosis. A possible link between the histological and clinical findings of candidiasis was indicated by a study that examined leukemic patients with renal candidiasis, that is, the peripheral leukocyte count correlated, to some extent, with the level of polymorphonuclear leukocyte infiltration into the sites of lesions. A similar correlation was observed in the present study in which lesions in CNS candidiasis were examined. The counts of peripher-

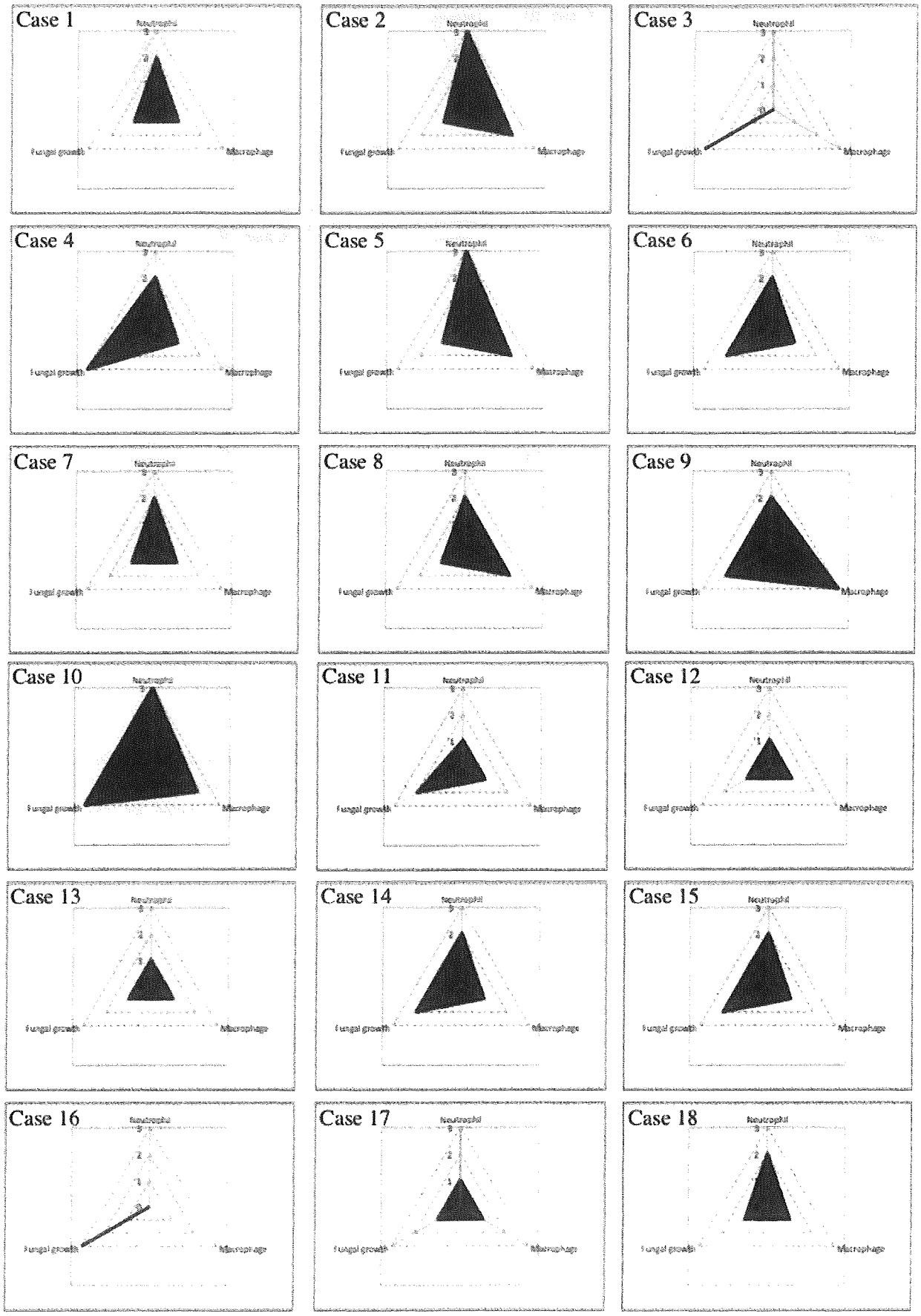

Fig. 10. Radar chart about tissue responses in all cases. (Case 1～Case 18)

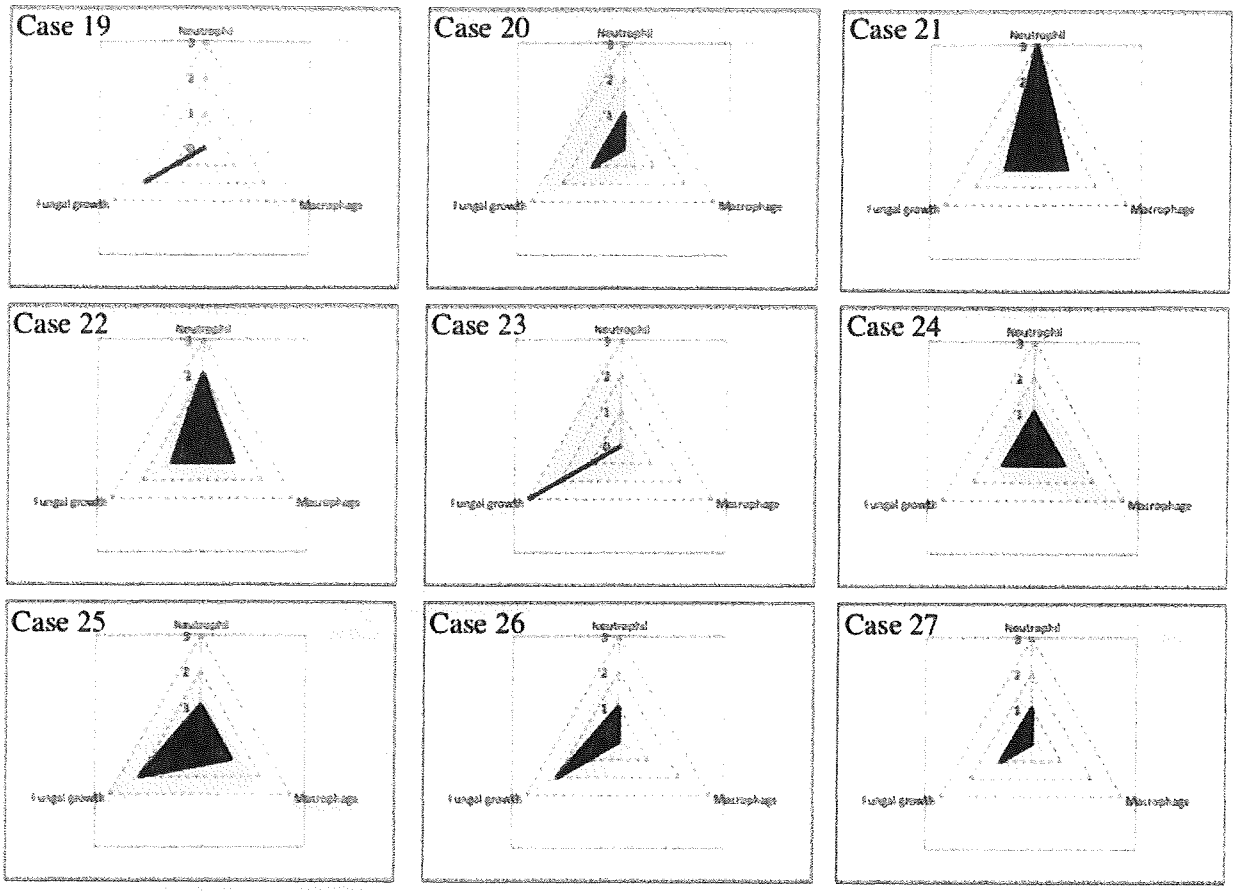

Fig. 10. Radar chart about tissue responses in all cases. (Case 19~Case 27)

al leukocyte at the end stage of the necrotic process were higher in patients with neutrophil-dominant lesions than in those with other types of lesions. Moreover, this study revealed that neutrophil infiltration was prominent in larger lesions developed in the supratentorial region, and that the level of neutrophil infiltration in a lesion was low when fungi were actively proliferating. These results support previous findings and further suggest that the brain, which was believed to be inert with respect to tissue reaction, directly indicates systemic tissue reaction.

Acknowledgments

This work was supported by the Health Science Research Grants for Research on Emerging and Reemerging Infectious Diseases (H16-Shinko-6 and H19- Shinko-8) and Measures for Intractable Diseases (H20 nannchi ippann35) from the Ministry of Health, Labour and Welfare of Japan, and by a grant of the Strategic Basis on Research Grounds for Non-governmental Schools at Heisei 20th from the Japanese Ministry of Education, Culture, Sports, Science and Technology to K. S.

We thank all the members of the 2nd Department of Neurosurgery and Department of Surgical Pathology, Toho University School of Medicine, for their collaboration.

References

1) Shibuya K, Paris S, Ando T, Nakayama H, Hatori T, Latgé JP: Catalases of *Aspergillus fumigatus* and inflammation in aspergillosis. Nippon Ishinkin Gakkai Zasshi **47**: 249-255, 2006.
2) Paris S, Wysong D, Debeaupuis JP, Shibuya K, Philippe B, Diamond RD, Latgé JP: Catalases of *Aspergillus fumigatus*. Infect Immun **71**: 3551-3562, 2003.
3) Kume H, Yamazaki T, Abe M, Tanuma H, Okudaira M, Okayasu I: Epidemiology of visceral mycoses in patients with leukemia and MDS - Analysis of the data in annual of pathological autopsy cases in Japan in 1989, 1993, 1997 and 2001. Nippon Ishinkin Gakkai Zasshi **47**: 15-24, 2006.
4) Yamazaki T, Kume H, Murase S, Yamashita E, Arisawa M: Epidemiology of visceral mycoses: analysis of data in annual of the pathological autopsy cases in Japan. J Clin Microbiol **37**: 1732-1738, 1999.
5) Pappas, PG: Invasive candidiasis. Infect Dis Clin North Am **20**: 485-506, 2006.

6) Pfaller MA, Diekema DJ: Epidemiology of invasive candidiasis: a persistent public health problem. Clin Microbiol Rev **20**: 133-163, 2007.
7) Sánchez-Portocarrero J, Pérez-Cecilia E, Corral O, Romero-Vivas J, Picazo JJ: The central nervous system and infection by *Candida* species. Diagn Microbiol Infect Dis **37**: 169-179, 2000.
8) Parker JC Jr, McCloskey JJ, Lee RS: Human cerebral candidosis-a postmortem evaluation of 19 patients. Hum Pathol **12**: 23-28, 1981.
9) Pendlebury WW, Perl DP, Munoz DG: Multiple microabscesses in the central nervous system: a clinicopathologic study. J Neuropathol Exp Neurol **48**: 290-300, 1989.
10) Hagensee ME, Bauwens JE, Kjos B, Bowden RA: Brain abscess following marrow transplantation: experience at the Fred Hutchinson Cancer Research Center, 1984 -1992. Clin Infect Dis **19**: 402-408, 1994.
11) Rigby S, Procop GW, Haase G, Wilson D, Hall G, Kurtzman C, Oliveira K, Von Oy S, Hyldig-Nielsen JJ, Coull J, Stender H: Fluorescence *in situ* hybridization with peptide nucleic acid probes for rapid identification of *Candida albicans* directly from blood culture bottles. J Clin Microbiol **40**: 2182-2186, 2002.
12) Altschul SF, Gish W, Miller W, Myers EW, Lipman. DJ: Basic local alignment search tool. J. Mol. Biol **215**: 403-410, 1990.
13) Kurtzman CP, Robnett CJ: Identification and phylogeny of ascomycetous yeasts from analysis of nuclear large subunit (26S) ribosomal DNA partial sequences. Antonie Leeuwenhoek **73**:331-371, 1998.
14) Falini B, Flenghi L, Pileri S, Gambacorta M, Bigerna B, Durkop H, Eitelbach F, Thiele J, Pacini R, Cavaliere A, Martelli M, Cardarelli N, Sabattini E, Poggi S, Stein H: PG-M1: a new monoclonal antibody directed against a fixative-resistant epitope on the macrophage-restricted form of the CD68 molecule. Am J Pathol **142**: 1359-72, 1993.
15) Garey KW, Rege M, Pai MP, Mingo DE, Suda KJ, Turpin RS, Bearden DT: Time to initiation of fluconazole therapy impacts mortality in patients with candidemia: a multi-institutional study. Clin Infect Dis **43**: 25-31, 2006.
16) Morrell M, Fraser VJ, Kollef MH: Delaying the empiric treatment of *candida* bloodstream infection until positive blood culture results are obtained: a potential risk factor for hospital mortality. Antimicrob Agents Chemother **49**: 3640-3645, 2005.
17) Lugert R, Schettler C, Gross U: Comparison of different protocols for DNA preparation and PCR for the detection of fungal pathogens in vitro. Mycoses **49**: 298-304, 2006.
18) Egholm M, Buchard O, Christensen L, Behrens C, Freier SM, Driver DA, Berg RH, Kim SK, Norden B, Nielsen PE: PNA hybridizes to complementary oligonucleotides obeying the Watson-Crick hydrogen bonding rules. Nature **365**: 556-568, 1993.
19) Stefano K, Hyldig-Nielsen JJ: Diagnostic applications of PNA oligomers. *In* Diagnostic gene detection & quantification technologies. IBC Library Series (Minden SA, Savage LM ed), pp.19-37, Southborough, Mass, 1997.
20) Stender H, Mollerup TA, Lund K, Petersen KH, Hongmanee P, Godtfredsen SE: Direct detection and identification of Mycobacte-rium tuberculosis in smear-positive sputum samples by fluorescence *in situ* hybridization (FISH) using peptide nucleic acid (PNA) probes. Int. J. Tuberc. Lung Dis **3**: 830-837, 1999.
21) Oliveira K, Hyldig-Nielsen JJ, Kurtzman C, Stender H: Differentiation between *Candida albicans* and *Candida dubliniensis* by fluorescence *in situ* hybridization using PNA probes. J. Clin. Microbiol **39**: 4138-4141, 2001.
22) Padilla A, Manterola JM, Rasmussen OF, Lonca J, Doninguez J, Matas L, Hernandez A, Ausina V: Evaluation of a fluorescence hybridization assay using peptide nucleic acid probes for identification and differentiation of tuberculous and non-tuberculous mycobacteria in liquid cultures. Eur. J. Microbiol. Infect. Dis **19**: 140-145, 2000.
23) Oliveira K, Procop GW, Wilson D, Coull J, Stender H: Rapid identification of Staphylococcus aureus directly from blood cultures by fluorescence *in situ* hybridization using PNA probes. J. Clin. Microbiol **40**:247-251, 2002.
24) Yao H, Yuzuriha T, Fukuda K, Marumoto T, Ibayashi S, Uchimura H, Fujishima M: Cerebral blood flow in nondemented elderly subjects with extensive deep white matter lesions on magnetic resonance imaging. J Stroke Cerebrovasc Dis **9**: 172-175, 2000.
25) Pendlebury WW, Perl DP, Munoz DG: Multiple Microabscesses in the Central Nervous System: A Clinicopathologic Study. Journal of Neuropathology & Experimental Neurology **48**: 290-300, 1989.
26) Omuta J, Uchida K, Yamaguchi H, Shibuya K: Histopathological study on experimental endophthalmitis induced by bloodstream infection with *Candida albicans*. Jpn J Infect Dis **60**: 33-39, 2007.
27) Akima M, Nonaka H, Kagesawa M, Tanaka K: A study on the microvasculature of the cerebral cortex. Fundamental architecture and its senile change in the frontal cortex. Lab Invest **55**: 482-489, 1986.
28) Nonaka H, Akima M, Hatori T, Nagayama T, Zhang Z, Ihara F: Microvasculature of the human cerebral white matter: Arteries of the deep white matter. Neuropathology **23**: 111-118, 2003.
29) Jong AY, Stins MF, Huang SH, Chen SH, Kim KS: Traversal of *Candida albicans* across Human Blood-Brain Barrier In Vitro. Infect Immun **69**: 4536-4544, 2001.
30) Nakamura M: the central nerves disease. *In* rinshoigakugairon 2nd ed (Knamamori I, Watabe Y, Ido Y, Haba K, Yasuda E, Onoki M ed), pp93, iryokagakusha, Tokyo, 2004.
31) Cheng K, Waggoner RA, Tanaka K: Human ocular dominance columns as revealed by high-field functional magnetic resonance imaging. Neuron **32**: 359-374, 2001.

Disseminated Aspergillosis Following Resolution of *Pneumocystis* Pneumonia with Sustained Elevation of Beta-Glucan in an Intensive Care Unit: a Case Report

T. Saito, N. Shime, K. Itoh, N. Fujita, Y. Saito, M. Shinozaki, K. Shibuya, K. Makimura, S. Hashimoto

Abstract
Invasive aspergillosis is a major cause of morbidity and mortality in immunocompromised patients receiving intensive care. The double-sandwich ELISA for galactomannan is reported to have a high sensitivity (96.5%) for the detection of invasive aspergillosis when a cut-off value of 0.8 ng/ml is used. However, we have experienced a case of lethal disseminated aspergillosis in a patient that presented with a negative galactomannan (GM) test and persistent elevation of β-D glucan (BG) levels. A 63-year-old female was admitted to our Intensive Care Unit (ICU) in acute respiratory failure and elevated BG. She had been receiving medication for Goodpasture syndrome based on anti-glomerular basement membrane antibodies and myeloperoxidase-antineutrophil cytoplasmic antibodies for 9 months and was receiving long-term prednisolone therapy (20 mg/day). On admission, her trachea was immediately intubated, and a PCR analysis of the bronchoalveolar lavage sample revealed *Pneumocystis jiroveci*. Trimethoprimsulfamethoxazole therapy was started for *Pneumocystis* pneumonia. The levels of BG remained elevated (> 100 pg/ml) during the treatment period despite the clinical resolution of *Pneumocystis* pneumonia, raising concerns of another complicated invasive fungal disease; consequently, fosfluconazole was administered empirically. The serum BG levels, however, did not decrease. Blood cultures did not detect a fungal infection. Serum GM levels measured by a double-sandwich ELISA on the 6th, 11th, and 24th days in the ICU were negative (< 0.2 ng/ml). The patient ultimately died of multiple organ failure on the 45th ICU day. Postmortem examination revealed a disseminated fungal infection with aggressive vascular invasion of the lungs, heart, and brain. In situ hybridization with a 568-bp probe of the alkaline proteinase sequence of *Aspergillus fumigatus* showed specific positive staining within the fungus present in the infected lung tissue, revealing that this patient may have had a systemic infection by *A. fumigatus* or *A. flavus*. This is a case of serum GM-negative disseminated aspergillosis pathologically proven by autopsy. Persistent elevated BG levels (> 100 pg/ml) refractory to trimethoprim-sulfamethoxazole and fosfluconazole may suggest possible *Aspergillus* infection and should prompt the initiation of empiric anti-aspergillosis therapies in patients at risk for fungal infection.

Infection 2009; 37: 547–550
DOI 10.1007/s15010-009-8108-5

Introduction

Invasive aspergillosis (IA) is a major cause of morbidity and mortality in immunocompromised patients receiving intensive care. The lung is the main portal of entry and is affected in 80–90% of cases of IA [1]. Disseminated aspergillosis (DA) is the most fulminant presentation of IA, diffusely involving multiple organ systems. The case-fatality rate of DA is as high as 88.1% [2], which strongly indicates the need for prevention or earlier diagnosis and treatment. The prevalence of IA is increasing in Japan and the USA [3, 4], but autopsy studies have revealed that the diagnosis of IA is commonly missed in Intensive Care Units (ICUs) [5].

A definition of invasive fungal infection has been developed [6, 7], but the early diagnosis of IA is still challenging. Good clinical culture samples are frequently unavailable, so clinicians have recently been utilizing several adjunctive diagnostic methods, such as the galac-

T. Saito *(corresponding author)*, **Y. Saito**
Division of Thoracic Surgery, Dept. of Thoracic and Cardiovascular Surgery, Kansai Medical University Hirakata Hospital, 2-3-1 Shin-machi, Hirakata, 573-1191, Japan; Phone: (+81/72) 804-0101, Fax: -2865, e-mail: saitotom@hirakata.kmu.ac.jp
N. Shime, S. Hashimoto
Dept. of Anesthesiology and Intensive Care, Kyoto Prefectural University of Medicine, Kyoto, Japan
K. Itoh
Dept. of Pathology and Applied Neurobiology, Graduate School of Medical Science, Kyoto Prefectural University of Medicine, Kyoto, Japan
N. Fujita
Dept. of Molecular Genetics and Laboratory Medicine, Kyoto Prefectural University of Medicine, Kyoto, Japan
M. Shinozaki, K. Shibuya
Dept. of Pathology, Toho University School of Medicine, Tokyo, Japan
K. Makimura
Dept. of Molecular Biology and Gene Diagnosis, Institute of Medical Mycology, Teikyo University, Tokyo, Japan

Received: March 15, 2008 · Revision accepted: March 2, 2009
Published online: September 2, 2009

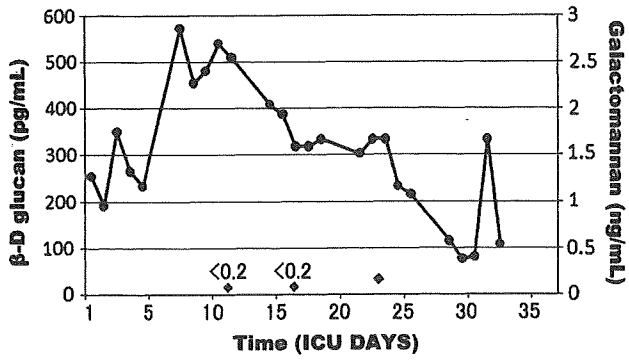

Figure 1. Kinetics of the (1 → 3)-β-D-glucan (BG; filled circles) and galactomannan (GM; diamonds) assays in this case. The GM levels were persistently negative (<0.2 ng/ml), whereas the BG concentration showed a sustained elevation (> 100 pg/ml) and resurged on the 31st ICU day.

tomannan (GM) antigen detection test or the (1 → 3)-β-D-glucan (BG) assay. The double-sandwich ELISA for the detection of GM is reported to have high sensitivity (96.5%) and high specificity (97.3%) for IA when a cut-off value of 0.8 ng/ml is used [8]. However, we have recently experienced a case of lethal DA in which the patient presented with a negative GM test and persistent elevated BG levels.

Case Presentation

A 63-year-old female was admitted to our ICU in acute respiratory failure with a decreased a PaO_2/FiO_2 (P/F) ratio < 200 and elevated BG (β-D glucan test Wako; Wako Pure Chemical Industries, Tokyo, Japan) and C-reactive protein levels. She had been receiving medication for Goodpasture syndrome with anti-glomerular basement membrane (GBM) antibodies and myeloperoxidase-anti-neutrophil cytoplasmic antibodies (MPO-ANCA) for 9 months, long-term prednisolone therapy (20 mg/day), and intravenous immunoglobulin infusion or intermittent hemodialysis. During the treatment period she had alveolar hemorrhage, cytomegalovirus (CMV) infection, duodenal ulcer, and crusted scabies.

On admission, her trachea was immediately intubated and bronchoalveolar lavage (BAL) was performed. A PCR analysis of the BAL sample revealed *Pneumocystis jiroveci*, and trimethoprim–sulfamethoxazole was started for *Pneumocystis* pneumonia (PCP). Her P/F ratio improved to 300 on the tenth day in the ICU, and the *P. jiroveci* became undetectable by PCR on the 23rd ICU day. The levels of BG, however, showed elevated (> 100 pg/ml) during the treatment period, despite clinical resolution of the PCP (Figure 1).

The high BG levels raised concerns of another complicated invasive fungal disease and, therefore, fosfluconazole was administered empirically. The serum BG levels, however, did not decrease. Blood cultures did not detect a fungal infection. Serum GM levels measured by double-sandwich ELISA (Platelia Aspergillus; Bio-Rad, Marnes La Coquette, France) on the 6th, 11th, and 24th ICU days were negative (< 0.2 ng/ml), and there was no prolonged neutropenia (< 500/mm^3 for > 10 days) during the ICU stay.

The patient subsequently developed *Pseudomonas aeruginosa* bacteremia and a CMV infection relapse, necessitating long-term antimicrobial therapy. She died of multiple organ failure on the 45th ICU day. Postmortem examination revealed a disseminated fungal infection with aggressive vascular invasion and abscess formation in the heart, brain, and lungs (Figiure 2a–c). In situ hybridization with a 568-bp probe of the alkaline

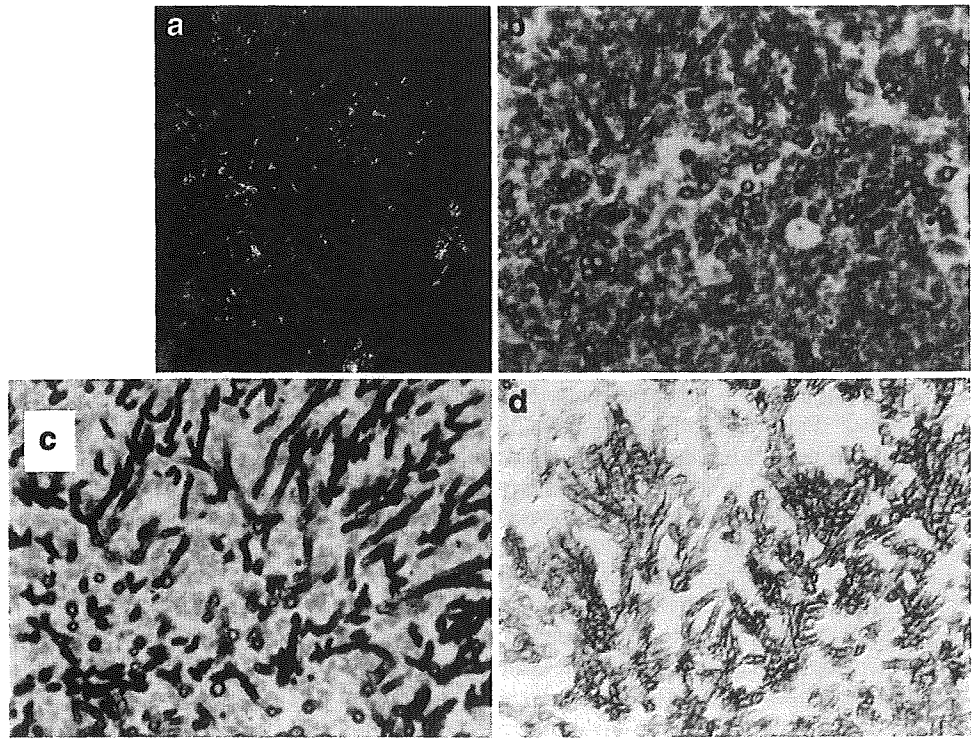

Figure 2. a) Macroscopic picture and microphotographs of lung tissue from the patient described here, b) an abscess formation on the surface of left upper lobe, c) hematoxylin–eosin staining, d) Grocott stain shows proliferating fungi with angioinvasion; DNA in situ hybridization with the alp-568 probe demonstrates specific signal within the same area.

proteinase sequence of *A. fumigatus* showed a specific positive staining within the fungus present in the infected lung tissue (Figure 2d), indicating that this patient may have had a systemic infection by *A. fumigatus* or *A. flavus*. Crescentic glomerulonephritis and pulmonary capillaritis was also found. *Pneumocystis jiroveci* was not found in the lungs.

Discussion

Here we report a rare case of autopsy-proven DA with false-negative GM test results. It has been reported that *A. fumigatus* and *A. flavus* can be detected in infected tissue by in situ hybridization with an alp-568-bp probe [9]. Our patient suffered from Goodpasture syndrome with MPO-ANCA and anti-GBM antibody, and such individuals are reportedly at high risk of severe infection [10].

GM is a polysaccharide cell-wall component that is released by *Aspergillus* spp during mycelial growth. The sandwich ELISA test recognizes (1 → 5)-β-D-galactofuranose side chains of GM with the EB-A2 monoclonal antibody [11]. The GM test has a high specificity and a wide range of sensitivity (30–100%) [12]. The major reasons for false-negative results are high cut-off values and exposure to antifungal agents [13]. Sensitivity can be improved to 96.5% when a cut-off of 0.8 ng/ml is used [8], but the serum GM levels were < 0.2 ng/ml in our case. Although antifungal drugs, such as amphotericin B, decrease the release of galactofuran antigens by reducing fungal angioinvasion in neutropenic rabbits [14], our patient ultimately developed DA with aggressive vascular invasion. Consequently, the administration of fosfluconazole did not have an effect on the expression of GM antigenemia.

The persistently negative GM levels in this case may have been due to the presence of *Aspergillus* spp antibody, which can interfere with the performance of the sandwich ELISA [9], although this is an unproven speculation. Another possibility is that this *Aspergillus* may secrete a GM antigen with only one galactofuranose epitope, which cannot be detected by the sandwich ELISA with EB-A2 [10].

Another interesting feature in this case is the dissociation of the two adjunctive fungal parameters, GM and BG. The BG, a polysaccharide component of fungal cell walls, is an adjunctive parameter suggesting possible deep mycosis, but it is nonspecific with respect to fungal species [15, 16]. BG is also a reliable marker for the diagnosis of *Pneumocystis* pneumonia [17]. It is also known that serum BG levels are elevated in patients undergoing hemodialysis with modified regenerated cellulose membranes, but we used synthetic polysulfone membranes, which do not affect the BG levels [18]. Retrospectively, the resurgence of BG on the 31st ICU day may have indicated the systemic *Aspergillus* infection. Thus, this case suggests that if the BG level does not change despite clinical and pathological improvement of *Pneumocystis* pneumonia, clinicians should consider the possibility of complicated fungal infections. Given the ineffectiveness of empirically administered fosfluconazole, we should have suspected invasive infection by fosfluconazole-resistant fungi, such as *Aspergillus* spp. Additional empiric treatment with, for example, polyenes, mold active azoles (such as voriconazole [19, 20]), or echinocandins should have been considered, especially given the greater risk of fungal infection presented by this patient due to persistent immunosuppression from long-term steroid and antimicrobial therapy.

Conclusion

We report a case of serum GM-negative disseminated aspergillosis pathologically proven by autopsy. Persistent elevation in the BG levels (>100 pg/ml) refractory to trimethoprim–sulfamethoxazole and fosfluconazole drug therapy may suggest possible *Aspergillus* infection and should prompt the clinician to initiate empiric anti-aspergillosis therapies in patients at risk for fungal infections.

Acknowledgments

We would express our gratitude to Dr. Tadaaki Hiruki for his English editing of this manuscript.

References

1. Denning DW: Invasive aspergillosis. Clin Infect Dis 1998; 26: 781–805.
2. Lin SJ, Schranz J, Teutsch SM: Aspergillosis case-fatality rate: systemic review of the literature. Clin Infect Dis 2001; 32: 358–366.
3. Yamazaki T, Kume H, Murase S, Yamashita E, Arisawa M: Epidemiology of visceral mycoses: analysis of data in annual of the pathological autopsy cases in Japan. J Clin Microbiol 1999; 37: 1732–1738.
4. Dasbach EJ, Davis GM, Teusch SM: Burden of aspergillosis-related hospitalization in the United States. Clin Infect Dis 2000; 31: 1524–1528.
5. Thomas CM, Neil SY: The relationship of pre mortem diagnosis and post mortem findings in a surgical intensive care unit. Crit Care Med 1999; 27: 299–303.
6. Ascioglu S, Rex JH, de Pauw BE, Bennett JE, Bille J, Crokaert F, et al. Defining opportunistic invasive fungal infection in immunocompromised patients with cancer and hematopoietic stem cell transplants: an international consensus. Clin Infect Dis 2002; 34: 7–14.
7. de Pauw BE, Patterson TF: Should the consensus guidelines' specific criteria for diagnosis of invasive fungal infection be changed? Clin Infect Dis 2005; 41: S377–S380.
8. Maertens J, Theunissen K, Verbeken E, Lagrou K, Verhaegen J, et al. Prospective clinical evaluation of lower cut-offs for galactomannan detection in adult neutropenic cancer patients and haematological stem cell transplant recipients. Br J Haematol 2004; 126: 852–860.
9. Hanazawa R, Yamagata S, Yamaguchi H: In situ detection of Aspergillus fumuigatus. J Med Microbiol 2000; 49: 285–290.
10. Levy JB, Hammad T, Coulthart A, Dougan T, Pusey CD: Clinical features and outcome of patients with both ANCA and anti-GBM antibodies. Kidney Int 2004; 66: 1535–1540.

11. Mennink-Kersten MA, Donnelly JP, Verweij PE: Detection of circulating galactomannan for the diagnosis and management of invasive aspergillosis. Lancet Infect Dis 2004; 4: 349–357.
12. Pfeiffer CD, Fine JP, Safdar N: Diagnosis of invasive aspergillosis using a galactomannan assay: a meta-analysis. Clin Infect Dis 2006; 42: 1417–1427.
13. Aquino VR, Goldani LZ, Pasqualotto AC: Update on the contribution of galactomannan for the diagnosis of invasive aspergillosis. Mycopathologia 2007; 163: 191–202.
14. Francis P, Lee JW, Hoffman A, Peter J, Francesconi A, et al. Efficacy of unilamellar liposomal amphotericin B in treatment of pulmonary aspergillosis in persistently granulocytopenic rabbits: the potential role of br onchoalveolar D-mannitol and serum galactomannan as markers of infection. J Infect Dis 1994; 169: 356–368.
15. Odabasi Z, Mattiuzzi G, Estey E, Kantarjian H, Saeki F, Ridge RJ, et al. β-D-Glucan as a diagnostic adjunct for invasive fungal infections: validation, cutoff development, and performance in patients with acute myelogenous leukemia and myelodysplastic syndrome. Clin Infect Dis 2004; 39: 199–205.
16. Pazos C, Ponto J, Del Palacio A: Contribution of (1 → 3)-β-D-glucan chromogenic assay to diagnosis and therapeutic monitoring of invasive aspergillosis in neutropenic adult patients: a comparison with serial screening for circulating galactomannan. J Clin Microbiol 2005; 43: 299–305.
17. Tasaka S, Hasegawa N, Kobayashi S, Yamada W, Nishimura T, et al. Serum indicators for the diagnosis of Pneumocystis pneumonia. Chest 2007; 131: 1173–1180.
18. Kato A, Takita T, Furuhashi M, Takahashi T, Maruyama Y, Hishida A: Elevation of blood (1 → 3)-beta-D-glucan concentrations in hemodialysis patients. Nephron 2001; 89: 15–19.
19. Herbrecht R, Denning DW, Patterson TF, Bennett JE, Greene RE, et al. Voriconazole versus amphotericin B for primary therapy of invasive aspergillosis. N Engl J Med 2002; 347: 408–415.
20. Walsh TJ, Pappas P, Winston DJ, Lazarus HM, Petersen F, et al. Voriconazole compared with liposomal amphotericin B for empirical antifungal therapy in patients with neutropenia and persistent fever. N Engl J Med 2002; 346: 225–234.

Aspergillus fumigatus and Aspergillosis
Edited by J.-P. Latgé and W. J. Steinbach

Chapter 27

Histology and Radiology

REGINALD GREENE, KAZUTOSHI SHIBUYA, AND TSUNIHIRO ANDO

Aspergillus fumigatus is a ubiquitous mold that causes a wide range of diseases in humans, each having characteristic imaging findings that reflect their defining histopathology and pathogenetic sequences. These illnesses can cause innocent saprophyte growth in preexisting chronic lung cysts, lead to allergic lung damage, or create life-threatening invasive infection. In some cases, the imaging findings simulate other serious infectious and noninfectious conditions, and in other cases the findings can even be confused with other categories of aspergillosis. The risk of developing one or another form of aspergillosis is strongly influenced by host factors, including the clinical background, the presence of preexisting underlying lung disease, and the patient's immune status. Other factors include the route of entry of the organism and the size of the inoculum. In this chapter the pathology of the three major categories of pulmonary aspergillosis (invasive, allergic, and saprophytic) and the diagnostic imaging challenges they pose are discussed (Greene, 1981; Soubani and Chandrasekar, 2002).

INVASIVE PULMONARY ASPERGILLOSIS

A. fumigatus rarely causes invasive infection in the immunocompetent host. In the severely immunocompromised host who is at high risk of invasive mold infection, however, it often causes life-threatening primary opportunistic fungal pneumonia. Because the common route of entry is characteristically via pulmonary ventilation, the lung is the most common initial site of infection (Herbrecht et al., 2002). Two unique pathogenetic sequences are responsible for acute invasive pulmonary aspergillosis (IPA). The first, and most important in clinical practice, is angio-invasion, which is responsible for >90% of such infections (Greene et al., 2007; Herbrecht et al., 2002). In this sequence, the infection initiates in the distal airspaces of what is often an otherwise-normal lung. In the second, much less common sequence, airway invasion, infection initiates in the more proximal bronchial airways in what is often previously injured or deformed cystic lung (Franquet et al., 2001). Chronic invasive aspergillosis is an uncommon but potentially life-threatening crossover entity that shares some aspects of both the saprophytic and acute invasive categories of pulmonary aspergillosis and needs to be carefully distinguished (Denning et al., 2003).

Angio-Invasive Pulmonary Aspergillosis

Acute angio-invasive aspergillosis primarily affects patients at high risk of invasive mold infection, in particular those severely immunocompromised by hematopoietic stem cell transplantation (HSCT) or hematologic conditions, particularly when associated with prolonged neutropenia or neutrophil dysfunction (Shibuya et al., 1997; Wakayama et al., 2002). The risk of dissemination and ultimately death are very high (Herbrecht et al., 2002). Among patients with T-cell-dominated immunodeficiency, e.g., solid organ transplant recipients and those with acquired immunodeficiency, the risk of angio-invasive pulmonary aspergillosis is much more sporadic and less common than in the two aforementioned high-risk groups.

Histopathology of early IPA

The histopathology of acute angio-invasive aspergillosis represents the net result of the interaction between the aggression of the invading mold and the host defense reaction to it. Initially, the characteristic lesion is a discrete nodule. It consists of central and peripheral parts: a central zone of coagulation necrosis, invading hyphal forms of *A. fumigatus*, and vascular thrombosis,

Reginald Greene • Dept. of Radiology, Massachusetts General Hospital, Harvard Medical School, Boston, MA 02114. Kazutoshi Shibuya and Tsunihiro Ando • Dept. of Surgical Pathology, Toho University School of Medicine, 6-11-1 Omori-Nishi, Ota-Ku, Tokyo 143-8541, Japan.

and a peripheral zone of hemorrhage (Fig. 1 and Color Plate 15). Classically, there is an absence of any associated inflammatory cellular infiltrate in this initial lesion, a characteristic that is attributable to severe neutropenia and/or neutrophil dysfunction (Shibuya et al., 1997, 1999b). The discrete nodule forms the basis for the analogous radiological halo sign, the earliest imaging indicator of angio-invasive aspergillosis.

Radiology of early IPA

By far the most common initial computed tomography (CT) finding of acute angio-invasive aspergillosis is the pulmonary macronodule or mass (≥1 cm diameter); at least one is present in about 90% of patients with IPA (Greene et al., 2007). The macronodule is such a common feature on initial CT of early angio-invasive aspergillosis that its absence argues against such a diagnosis (Greene et al., 2007). At times, nodules less than 1 cm in diameter may be encountered in acute angio-invasive IPA, but generally by the time clinical suspicion warrants a CT scan the nodule is ≥1 cm. The differential diagnosis of the macronodule is wide and includes infections and noninfectious processes by fungi, nocardiosis, tuberculosis, bacterial lung abscess, septic emboli, bland pulmonary infarcts, lung cancer, metastases, lymphoproliferative disorders, and vasculitis.

The halo sign is a special CT finding consisting of the constellation of a macronodule and a perimeter of ground-glass opacity (Fig. 2). In immunocompromised patients at very high risk of invasive mold infection, the halo sign has long been considered an early sign of IPA. On initial CT imaging this finding can be identified in a significant fraction of patients with IPA. In a large series of patients with IPA in whom the halo sign was a criterion for a probable diagnosis of IPA, it was identified in about 60% of all patients with IPA (Greene et al., 2007). The ground-glass component of the halo sign corresponds to hemorrhage surrounding the edge of the discrete nodule identified on histopathology (Shibuya et al., 2006). This sign is highly transitory. For instance, in one longitudinal CT study of patients with IPA in whom 72% of patients had a halo sign on initial CT, only 22% still had a detectable halo sign 10 days later (Caillot et al., 2001).

Differential diagnosis

False-positive halo signs may be produced by edge irregularities of nodules, by technical partial volume ef-

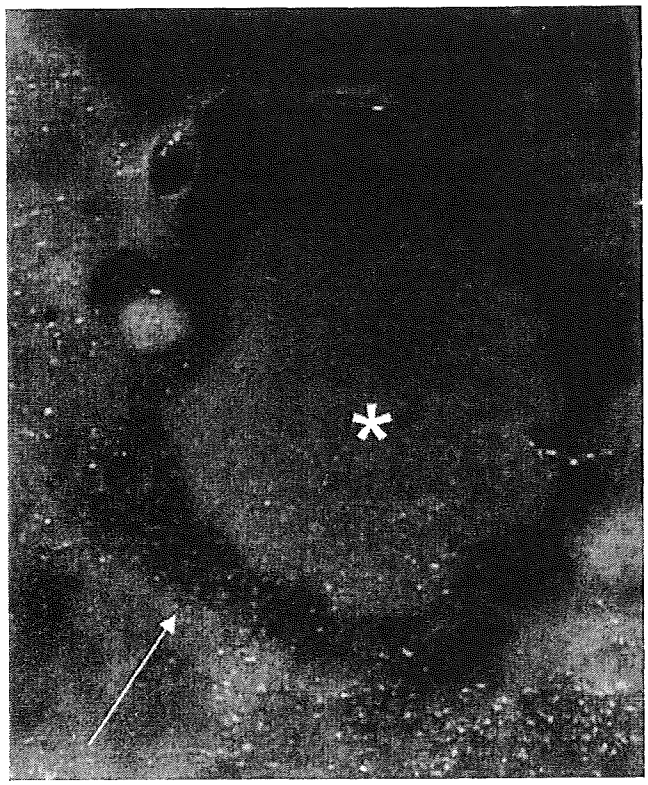

Figure 1. Histopathology of a discrete nodule in IPA. A sharply demarcated nodule (*) surrounded by hemorrhage (arrow) in a whole-lung section of a patient with angio-invasive aspergillosis.

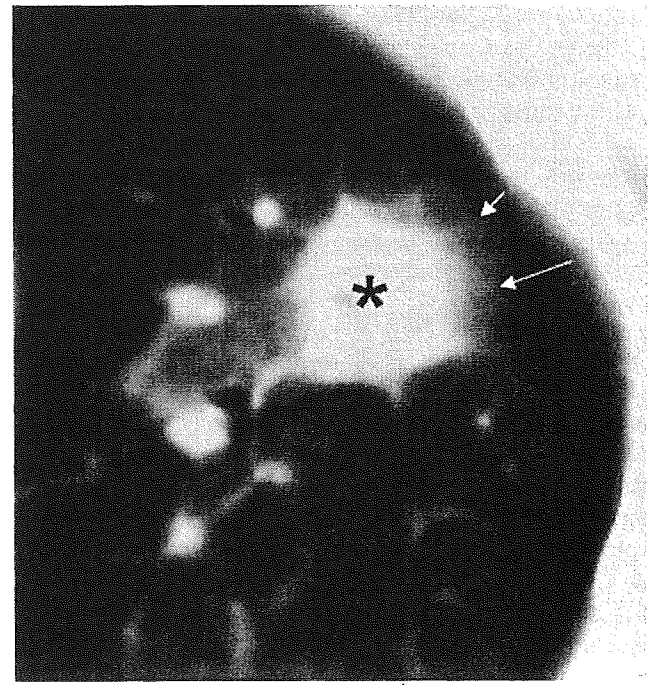

Figure 2. CT halo sign in IPA. The CT image of the lung demonstrates a halo sign in a patient with IPA and underlying hematological malignancy. The sign consists of two parts: first, a solid soft tissue macronodular core (≥1 cm) through which no pulmonary parenchyma is visible (*), and second, a ground-glass perimeter of intermediate density (arrows) through which the pulmonary parenchyma is still visible. Image obtained from Greene et al. (2007) with permission of the publisher.

fects that occur when CT sections are too thick for the size of the pulmonary nodules studied, and when respiratory motion degrades the images.

The CT halo sign is not unique to IPA. It has been reported in other less common angio-invasive mold infections, such as with *Zygomycetes* and even more rare angio-invasive fungi, e.g., *Trichosporon* spp., *Penicillium* spp., and *Fusarium* spp. (Huang and Harris, 1963; Saul et al., 1981; Young et al., 1978). Like *A. fumigatus*, these fungi can also produce nodular metastatic infectious nodules in solid abdominal organs like the liver and spleen, similar to those produced in chronic candidiasis. The halo sign has also been reported in a wide variety of other infections, such as those due to *Coccidioides immitis* and *Candida* spp., *Nocardia* spp., *Mycobacterium tuberculosis*, cytomegalovirus, herpes simplex virus, and angio-invasive bacteria, particularly *Pseudomonas aeruginosa* (Armstrong et al., 1971). Noninfectious conditions also associated with the halo sign include bronchio-alveolar cell carcinoma, lymphoproliferative disorders, metastatic angiosarcoma, Kaposi sarcoma, Wegener granulomatosis, eosinophilic lung disease, and organizing pneumonia (Gaeta et al., 1999; Kim et al., 1999; Primack et al., 1994). While there is a wide variety of conditions other than IPA that are associated with the CT halo sign, it is important to recognize that in the HSCT recipient, or the patient with a hematologic malignancy and neutropenia with suspected mold infection, angio-invasive aspergillosis is by far the most common cause of the CT halo sign.

Some studies indicate that preemptive anti-*Aspergillus* therapy based on the finding of a halo sign can improve outcome in patients with a compatible illness who are at high risk of invasive mold infection (Blum et al., 1994; Caillot et al., 1997). In an analysis of 235 patients with IPA who had an initial chest CT scan, 222 patients presented with at least one macronodule (Greene et al., 2007). Of the 143 of these patients who had an identifiable halo sign and the 79 who had no identifiable halo sign, a significantly higher satisfactory response rate at 12 weeks, irrespective of the treatment arm, was achieved in those with a halo sign (52% versus 29%). Those with halo signs also had better survival rates than those in the no-halo sign group (71% versus 53%) (Greene et al., 2007) (Fig. 3). Favorable treatment response in the halo sign group held true irrespective of the underlying condition category (hematological conditions or nonhematological conditions, baseline neutropenia or no baseline neutropenia, and allogeneic HSCT or no HSCT) (Greene et al., 2007). Since the improved outcome in the halo sign group is arguably related to the earlier stage of the infection as represented by the halo sign, the need for prompt performance of CT scanning and initiation of early preemptive treatment warrants a high priority when the sign is identified in such patients. The evanescent nature of the halo sign further emphasizes the urgency of obtaining a CT scan at the earliest opportunity when mold infection is first suspected.

Histopathology of Late IPA

The characteristic delayed (or transition) lesion of angio-invasive pulmonary aspergillosis occurs after partial recovery of neutrophil function, by which time the discrete nodule has begun to develop liquefaction necrosis limited to its periphery. This process is made possible by blood vessels around the margin of the discrete

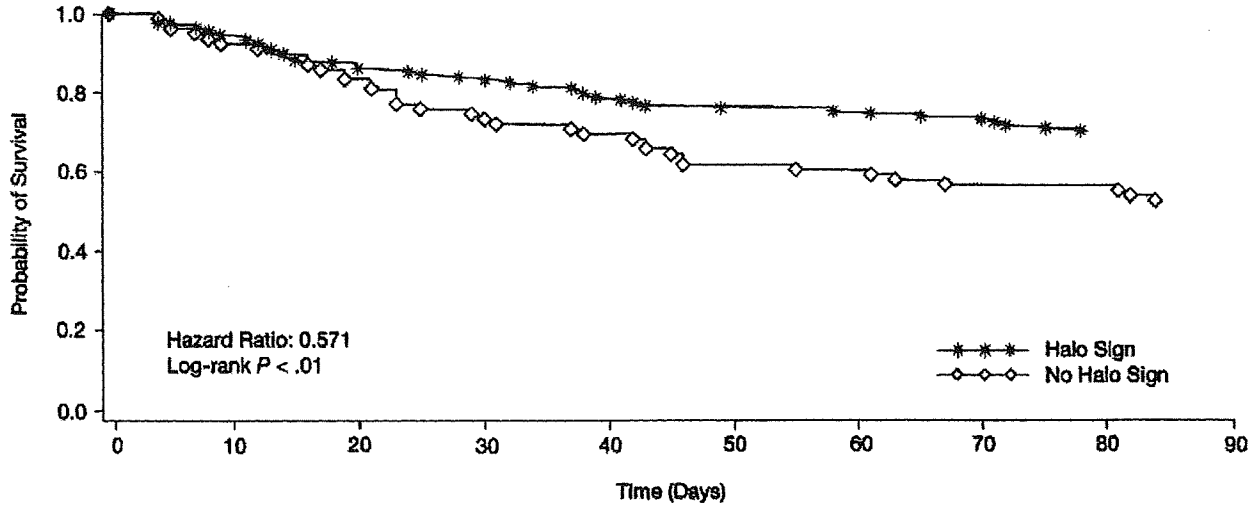

Figure 3. Time to death for patients under treatment for IPA who had a halo sign at presentation (n = 143) or without a halo sign at presentation (n = 79). Reprinted from Greene et al. (2007) with permission of the publisher.

nodule that remain patent. Thus, new neutrophils begin to be delivered to the nodule periphery, thereby facilitating liquefaction necrosis (Color Plate 16). The resulting cavitation separates the lung at the periphery of the persisting central zone of coagulation necrosis. The histopathology of this delayed transition lesion forms the basis for the analogous radiological "air crescent sign," an imaging indicator of late angio-invasive aspergillosis.

Radiology of late IPA

The air crescent sign is a specific type of cavitary lesion in which a semilunar pocket of gas surmounts a macronodule (Curtis et al., 1979) (Fig. 4). Since the appearance of the sign is generally known to coincide with recovery of neutrophil function, it is not surprising that it is found as an initial CT finding in only a small fraction of patients with IPA (~10%) (Greene et al., 2007). Like the halo sign, the air crescent sign is considered a specific indicator of IPA in patients at high risk of invasive mold infection (Aquino et al., 1994; Gefter et al., 1985). One investigation of patients with IPA reported that in the 4- to 10-day period following initial chest CT scan, while the frequency of the halo sign was rapidly diminishing, the frequency of the air crescent sign slowly increased (Caillot et al., 2001). Thick-walled and thin-walled cavities without air crescents can be found in a minority of initial CT studies of patients with IPA, but these findings do not seem to have the same diagnostic predictive value as the air crescent sign, from which they should be differentiated (Godwin et al., 1980).

Differential diagnosis

The differential diagnosis of the air crescent sign is broad, but like the halo sign, angio-invasive aspergillosis is the most common cause when it is found in a patient at high risk of invasive mold infection. The sign can also be found in a variety of other conditions, e.g., nocardiosis, tuberculosis, bacterial lung abscess, cavitary hematoma, and cavitary lung cancer (Ryu and Swensen, 2003; Tuncel, 1984). The nodule of coagulation necrosis in an air crescent sign cavity can closely resemble the fungus ball of saprophytic aspergillosis in a preexisting cyst. The unique clinical circumstances of each of these two patient groups help to differentiate the air crescent sign of IPA from the similar sign of aspergilloma. The two have very different histopathologies and pathogenesis: a patient with one is likely to be clinically well, while a patient with the other condition is likely to be very sick and at high risk of invasive mold infection.

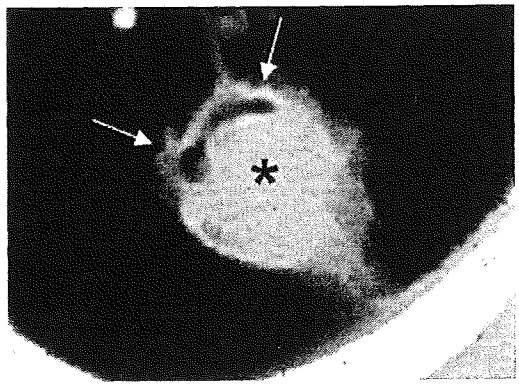

Figure 4. CT air crescent sign in IPA. The CT image demonstrates an air crescent sign in a patient with angio-invasive pulmonary aspergillosis and underlying hematological malignancy. A crescent of air (arrows) surmounts a soft tissue mound of a macronodule (*).

Other less common initial CT imaging findings in IPA include consolidations, consolidative infarcts with or without air bronchograms (about one-third of patients), and small airway opacities (about 1/10 of patients) (Greene et al., 2007). Ancillary CT findings, such as pleural effusion, pericardial effusion, and hilar/mediastinal lymphadenopathy, have not proved to be discriminatory.

The search for a CT halo sign-equivalent finding with magnetic resonance (MR) imaging has been disappointing. Early in the course of IPA, MR performs well with regard to sensitivity. However, specificity is poor and not improved by imaging after intravenous gadolinium (Gd) administration (Blum et al., 1994). On the other hand, with MR imaging later in the course of IPA, i.e., 10 days after onset, there is Gd-diethylenetriamine penta-acetic acid enhancement that often demonstrates a rim area with a characteristic nodular target-like lesion and a "reverse target" on T2-weighted images. These findings are highly suggestive of the later stage of IPA and are not found earlier in the course of disease or in patients with *Pseudomonas* sp. or staphylococcal infection.

Invasion into the great vessels pleura and pericardium, hila, and mediastinum occur relatively infrequently in IPA, but the consequences can be disastrous. If IPA lung lesions abut a large vessel, the possibility of such vessel invasion must be considered. Occasionally, hyphal elements invade adjacent large vessels to cause thrombosis or pseudoaneurysm; these developments increase the risk of blood-borne dissemination, vessel rupture, and exsanguination.

Cerebral aspergillosis generally occurs by direct extension from sino-nasal aspergillosis or systemic hematogenous dissemination from a primary lung infection. Initial brain lesions are analogous in appearance to those in the lung; they are usually well-defined macronodular lesions of low CT attenuation or large-vessel infarcts surrounded by edema. On MR imaging, cerebral lesions usually appear as T2-weighted hyperintense lesions sur-